Design and Mechanical Analysis of a Single-layer Common Coil Dipole for VLHC

I. Novitski, N. Andreev, G. Ambrosio, P. Bauer, V. V. Kashikhin, A.V. Zlobin.

Abstract— **Fermilab is developing a 2-in-1, 11 T block-type common coil dipole magnet for a future Very Large Hadron Collider. The common-coil design concept allows a large bending radius at the coil ends and therefore is well suited for use of the react-and-wind technique with brittle superconductors. The magnet features one-layer flat Nb_3Sn coil wound using pre-reacted cable. A novel mechanical design has been developed to provide effective coil support against Lorentz forces, minimize conductor displacement during excitation, reduce coil pre-load at room temperature, and prevent force accumulation. The details of the design concept and results of the mechanical analysis are presented in this paper.**

***Index Terms*—common coil dipole, mechanical design, superconducting accelerator magnet.**

I. Introduction

FERMILAB is working on the development of 10-12 T Nb_3Sn magnets for a Very Large Hadron Collider (VLHC), exploring different designs and fabrication techniques. One of the interesting approaches suitable for a react and wind technique is the block-type common-coil dipole magnet [1]. This approach offers some simplifications in magnet fabrication and a possibility to use brittle superconductors, in particular pre-reacted Nb_3Sn cable.

Several designs of the high field dipole magnet for VLHC based on this concept have been recently proposed [2,3]. A common feature of all those designs is a multi-layer/multi-block coil structure utilizing different cables. The mechanical analysis revealed serious mechanical problems in these designs [4, 5], in particular, large turn displacements during magnet excitation, high stress concentrations in the coil and the mechanical structure. To resolve these problems a variant with a horizontal split yoke was studied, resulting in low stress in the coils but introducing complicated yoke configuration and assembling technique [6]. This ultimately leads to complications of the magnet fabrication and eliminates the main advantage of the common coil approach – its simplicity. Note that the common coil design is not the most efficient from the viewpoint of conductor utilization.

To overcome these difficulties a single-layer common coil design with strong internal support structure has been developed at Fermilab [7]. This design preserves all the advantages of the common coil approach including a possibility to use a react and wind technique, fabrication simplicity and also provides the aperture size, maximum field, field quality and coil volume comparable to the cos-theta design. This paper presents a description of the proposed magnet design and the fabrication technology, and reports the results of a 2D mechanical analysis.

Manuscript received September 18, 2000.

This work was supported by the U.S. Department of Energy.

I. Novitski, N. Andreev, G. Ambrosio, P. Bauer, V. V. Kashikhin and A.V. Zlobin are with Fermilab, MS 316, Batavia, IL 60510 USA (telephone: (630) 840-4823, e-mail: novitski@fnal.gov)

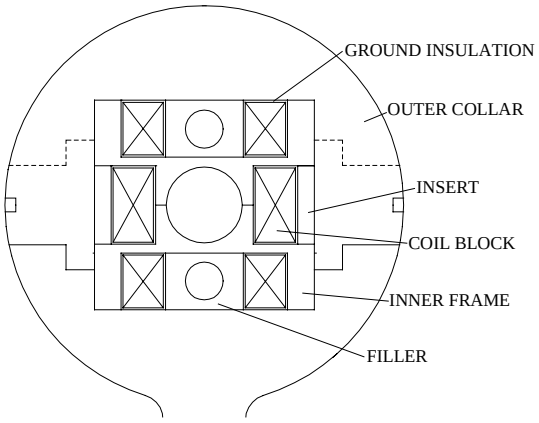

Fig. 1. Cross-section of the coil support structure.

II. Magnet Design and Fabrication

The magnet design is based on a single-layer flat racetrack coils with shifted pole blocks [7] shared between two apertures. The coils are made of reacted rectangular Rutherford-type cable with 60 Nb_3Sn strands, each 0.7 mm in diameter. The bare cable width is 21.09 mm and the thickness is 1.245 mm. The insulation is 0.10 mm thick and made of fiberglass tape. Each coil consists of 56 turns grouped into three blocks and separated by 6 mm thick spacers. There are also two 3 mm thick spacers in each middle block. The pole blocks are shifted horizontally inwards by 5 mm with respect to the middle blocks. The size and position of blocks and spacers were optimized to provide the maximum transfer function, minimum coil volume and small low-order geometrical harmonics within the largest possible gap. There is only one splice connecting the left and right coil in series. The gap between pole blocks is 40 mm, determining the magnet aperture. The use of the reacted Nb_3Sn cable dictates the minimum bending radius of 90 mm for the chosen strand size and thus sets the aperture separation to 280 mm.

The single-layer coil design with small number of current blocks separated by large spacers allows the use of a stress management strategy. Coil blocks, surrounded by the 0.5 mm thick electrical insulation, are placed inside a strong frame as shown in Fig.1. The frame has rectangular windows for the coil blocks and round holes for the beam pipe and the cooling

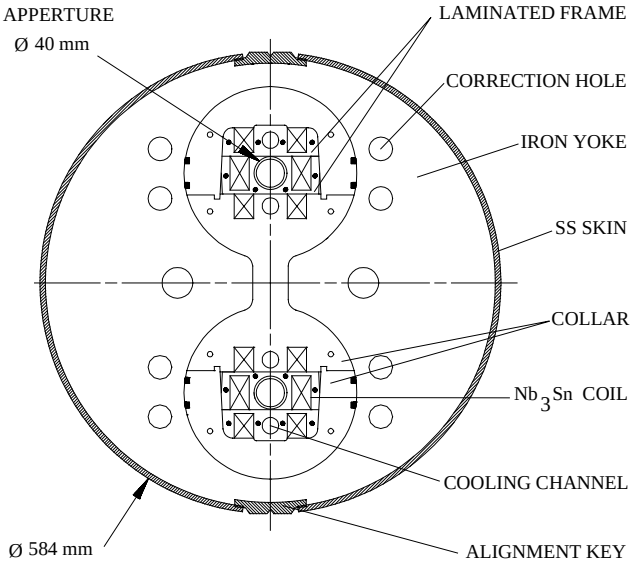

Fig. 2. Magnet design for one layer concept.

apertures and protects the coil from the horizontal and vertical over-compression. During operation the frame prevents an accumulation of the vertical component of Lorentz forces and force transfer from the pole blocks to the mid-plane block. It also intercepts a significant part of the horizontal component of Lorentz forces applied to the left and right coils and directed outward, reducing the force transferred to the yoke and skin.

The internal frame is surrounded by the external collar structure, which is common for both apertures. Keys or rods are used to lock the collars together. The collared coil assembly is placed inside the vertically split iron yoke surrounded by a 10 mm thick stainless steel skin. Thick end plates welded to the skin are used to restrict the longitudinal motion of the coils. The 2D cross-section of the magnet cold mass is shown in Fig.2.

The vertical prestress on the coils is supplied by the collars. The horizontal pre-compression of the collared coil is provided by the stainless steel skin via the iron yoke.

The design solutions described above result in some obvious fabrication steps and conditions. In particular, both coils are to be wound simultaneously and directly into the support structure. In order to do this the frame is divided into small components (called bridges) made of stainless steel laminations (see Fig.2). After winding, the collared coil assembly is impregnated with epoxy, which produces a very rigid monolithic mechanical structure. Kapton layers with mould release are used on the coil/frame interfaces as shear relief layers.

III. Mechanical Analysis

A mechanical analysis has been performed to verify the design concept, to optimize major dimensions and to choose structural materials. The criteria was that the maximum stress in the coil should be less than 150 MPa at all conditions, major structural elements should operate in the elastic regime and the turn motion in the operating field range of 0-11 T should not exceed 100 microns.

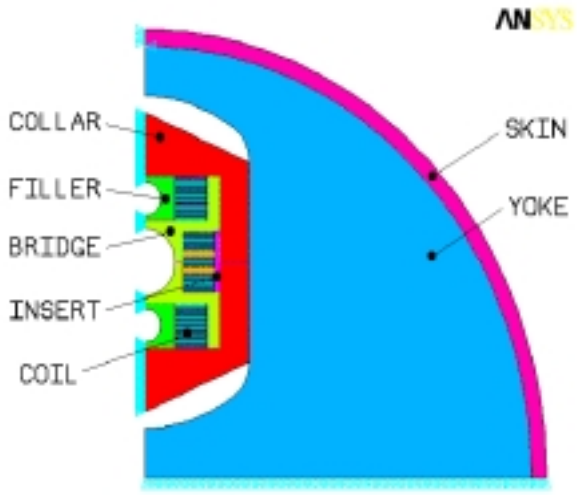

Fig. 3. Finite element model.

A. Finite Element Model

A 2D ANSYS® model has been developed and is shown in Fig.3. It consists of the following major elements: the coil blocks surrounded by 0.5 mm thick Kapton insulation, stainless steel (SS) frame, the 20 mm wide outer collars made of stainless steel or aluminum (Al), the iron yoke and the 10 mm thick stainless steel skin. The collar structure in the model has been simplified to avoid a model complication. For the same reason and taking into account the symmetry of the design only a quarter of the magnet cross-section is implemented. The model was meshed using elements PLANE2 and PLANE82 from the ANSYS® library. All interfaces have contact element type COMBIN40 without friction.

B. Electromagnetic Force

Lorentz forces for a magnetic field of 11 T in the aperture were computed using ROXIE [8] and ANSYS® codes. Fig. 4 shows the force distribution in the coil cross-section at that field.

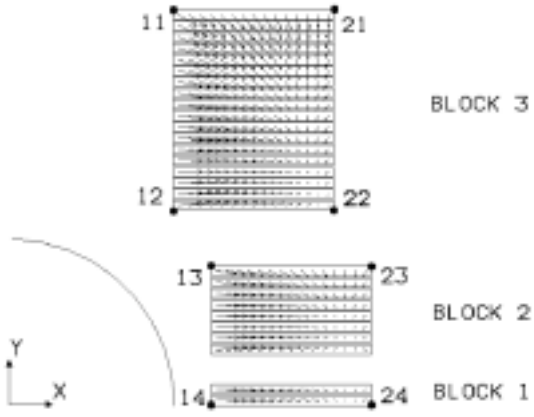

Fig. 4. Distribution of electromagnetic forces in the coil.

TABLE I
ELECTROMAGNETIC FORCES IN CONDUCTOR BLOCKS

Block Number	F_X [kN/m]	F_Y [kN/m]
1	185.7	-24.6
2	773.9	-227.6
3	1989.7	-1213.7
Total	2949.3	-1465.8

Table I presents the total electromagnetic forces for the three conductor blocks in one octant. The small difference in force level and asymmetry in their distribution in top and bottom parts of the coil was also taken into account in this analysis.

C. Material Properties

Table II summarizes the thermal and mechanical properties of the materials used in the model [9]. Since the coil is wound into the support structure and impregnated at low compression the low value for E_Y of 20 GPa was used.

TABLE II
MATERIAL PROPERTIES FOR THE FINITE ELEMENT CALCULATIONS

Material	Elasticity Modulus [GPa]				Thermal contraction 300 - 4.2 K [mm/m]	
	300 K		4.2 K			
	E_X	E_Y	E_X	E_Y	A_X	A_Y
Nb_3Sn coil	38	20	38	20	2.7	3.6
Copper	120	120	135	135	3.4	3.4
Al	70	70	85	85	4.1	4.1
SS 316LN	190	190	210	210	3.0	3.0
SS Nitronic 40	190	190	210	210	2.6	2.6
Iron	190	190	210	210	2.0	2.0
Kapton®	2.8	2.8	7	7	13	13

IV. RESULTS AND DISCUSSION

The following stages were analyzed:

- magnet assembly and coil prestress at 300 K
- magnet cool down from 300 to 4.2 K
- magnet excitation at 4.2 K to the nominal field of 11 T

The vertical pressure in the coil at room temperature was generated by a 0.1 mm interference at the collar/coil boundaries of block 3. The horizontal pre-compression of the collared coil was provided by the skin weld shrinkage of 0.2mm. Cool down from 300 to 4.2 K was modeled as an additional shrinkage of all structural materials. The electromagnetic forces were applied as a nodal load at 4.2 K.

Calculations were performed for two collar materials: aluminum and stainless steel. The main advantage of Al collars is the large thermal contraction that increases the coil prestress after cooling down as well as its low cost and simplicity of collar stamping. However, the results of calculations showed that the maximum equivalent stress in Al collars exceeds its yield stress value by a factor of two for the chosen collar dimensions. To reduce the stress a significant increase of the collar size is required.

The calculated distributions of equivalent stress in the coil with SS collars at 300 K, after cooling down and at the nominal field of 11 T are presented in Fig.5. The scale of stress in Fig.5-7 is given in units of kg/mm^2=10 MPa.

The stress distribution in the coil support structure (frame and SS collars) and reactions on the coil/frame and coil/collar

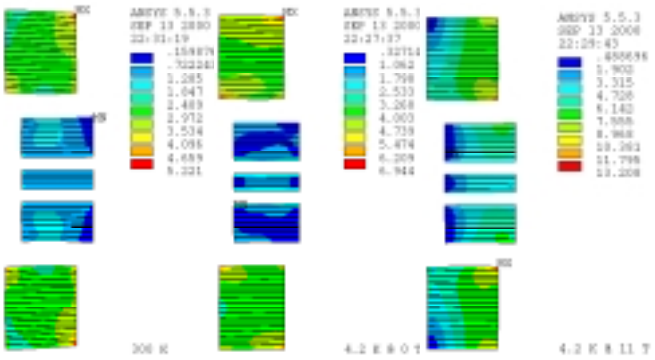

Fig. 5. Stress distribution in the coil at 300 K and 4.2 K before excitation and at nominal field of 11 T.

interfaces at 300 K and 4.2 K/11 T are shown in Fig.6. As it can be seen, the distribution of stress in the coil support structure at room and at operation temperature is not uniform. At room temperature the maximum value is located in the external collar, at helium temperature at nominal operation field the high stress region moves into the frame.

The distribution of nodal reactions shows the stress level on different interfaces. Table III summarizes coil average stress at different conditions on different coil surfaces calculated for SS collars.

TABLE III
AVERAGE COIL STRESS, [MPA]

Stage	Coil surface						
	11-21	12-22	13-23	11-12	21-22	13-14	23-24
300 K	31	31	11	17	17	1	1
4.2 K/ 0 T	28	28	4	41	41	5	5
4.2 K/11T	13	58	12	0	75	0	51

At room temperature the pole blocks are pre-compressed almost uniformly in vertical and horizontal directions. The middle block has lower, mostly vertical pre-compression. At helium temperature for the maximum Lorentz force there is no coil reaction (stress) on the left vertical interface between the coil blocks and the internal support structure. On the right interface it is almost uniformly distributed. Comparison of this reaction distribution with the reaction distribution on the collar yoke interface qualitatively shows the effectiveness of

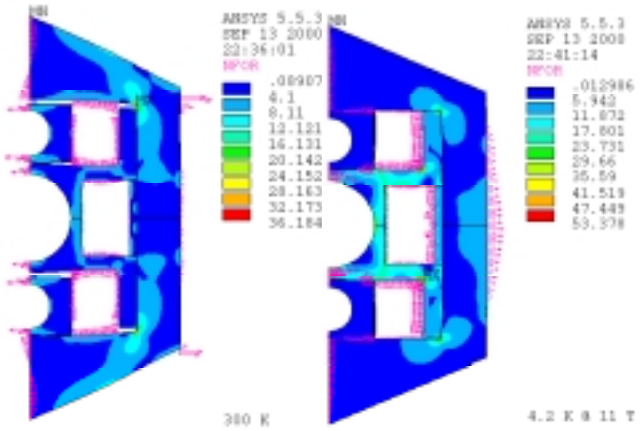

Fig. 6. Stress distribution in the frame and SS collars and nodal reactions on the coil/frame and coil/collar interfaces at 300 K and 4.2 K/11 T.

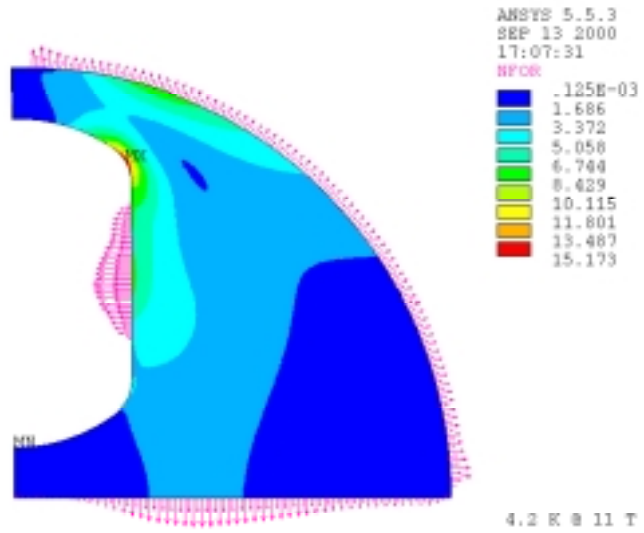

Fig. 7. Stress distribution in the yoke and nodal reactions on the yoke boundaries at 4.2 K and 11 T.

the internal support structure (frame) in confining the horizontal component of the Lorentz force. A comparison of the vertical reaction on the coil/frame interface for the pole block and middle block shows that the internal support structure prevents accumulation and transfer of the vertical component of the Lorentz force from one block to another.

Stress distribution in the yoke and nodal reactions on the yoke boundaries at 4.2 K and 11 T are shown in Fig.7. The distribution of stress in the yoke is not uniform. The maximum stress region is located near the boundary between the collars and yoke. The radial force on the yoke and skin boundary is uniform resulting in uniform azimuthal stress distribution in the skin.

Table IV summarizes the maximum equivalent stresses in the coil and major elements of mechanical support structure for the SS collars at room temperature and at operation temperature. As it can be seen, the maximum equivalent stresses in all parts of the magnet at all conditions are less than target design values.

TABLE IV
EQUIVALENT STRESS IN MAGNET DESIGN, [MPA]

Stage	coil	collar	frame	yoke	skin
300 K	52	361	118	99	125
4.2 K/ 0 T	69	408	178	194	327
4.2 K/11T	132	455	533	152	358

Table V summarizes the vertical and horizontal displacements of corner points of current blocks for different boundary conditions and prestress of the coil. In the first case the boundary between the coil and support structure is glued, and the last two cases allow a free motion of the coil blocks relative to the support structure.

For the glued coil/collar and coil/frame boundaries case the coil shape practically follows the shape of the support structure and the displacements are quite small. However, the shear stress on some coil boundaries exceeds 50 MPa, which is critical for the epoxy with shear strength of 30 MPa [10].

TABLE V
CONDUCTOR DISPLACEMENT UNDER LORENTZ FORCES, [μm]

Position	Impregnated structure w/o prestress		Free coil boundary w/o prestress		Free coil boundary with prestress	
	vertical	horizontal	vertical	horizontal	vertical	horizontal
11	-26	14	-91	36	-40	36
12	-12	17	-31	38	-9	32
13	-8	20	-5	66	-6	65
14	0	37	0	59	0	61
21	-17	15	-71	30	-28	30
22	-10	22	-32	35	-9	34
23	-7	24	-3	48	-2	46
24	0	29	0	53	0	52

For that reason a stress relief layer is needed, in particular for the coil boundaries 11-21, 11-12, 13-14, 13-23.

In both cases with free (sliding) boundaries between the coil and the support structure, the horizontal displacements are the same with or without the coil prestress, and they do not exceed 70 μm. A small vertical coil prestress of 30 MPa reduces the vertical displacements of pole block boundaries by a factor of 2-3 to the level of 30-40 μm. Such displacements are acceptable from the viewpoint of variation of field harmonics in the operation cycle and of magnet quench performance.

V. CONCLUSION

The mechanical design of the common coil dipole magnet for VLHC based on a single-layer coil and the pre-reacted Nb_3Sn cable has been developed. Results of mechanical analysis confirmed that the design meets all the target mechanical requirements including low stress in the coil and major elements of the mechanical structure as well as small turn motion in the operating field range.

REFERENCES

[1] G. Danby et al., "Pannel Discussion of Magnets for a Big Machine", Proc. of the 12th International Conf. On High-Energy Accelerators, Fermilab, August 11-16, 1983, p.52.

[2] R. Gupta, S. Ramberger, S. Russenschuck, "Field Quality Optimization in a Common Coil Magnet Design", IEEE Trans. on Appl. Superconductivity, v. 10, No 1, March 2000.

[3] G. Sabbi et al., "Conceptual Design of a Common Coil Dipole for VLHC", IEEE Trans. on Appl. Superconductivity, v. 10, No. 1, March 2000.

[4] I. Novitski, "Mechanical Analysis of the HFM with Common Coil Design", unpublished, FNAL/LBNL videoconference, November 1999.

[5] P. Bauer el al., "2D Mechanical Analysis of the Coil Package of the 1st FNAL Nb3Sn Common Coil Dipole Magnet", Technical Division Note, TD-00-015, February 2000.

[6] I. Novitski, "HFM Common Coil Dipole with Horizontally Split Yoke", Fermilab, Technical Division Note, TD-00-029, May 2000.

[7] V. Kashikin, A.V. Zlobin "Magnetic Designs of Fermilab 2-in-1 Nb3Sn Dipole Magnets for VLHC", presented at this conference.

[8] S. Russenschuck, "A computer program for the design of superconducting accelerator magnets", CERN AT/95-39, 1995.

[9] D.R. Chichili et al., "Investigation of cable insulation and thermo-mechanical properties of epoxy impregnated Nb3Sn composite", IEEE Trans. on Appl. Superconductivity, v. 10, No. 1, March 2000.

[10] S. Ohira, S. Nishijima, "Effect of impregnating material failure on stability of superconducting magnet analyzed by wire dynamics simulation", IEEE Trans. on Appl. Superconductivity, v. 10, No. 1, March 2000.